

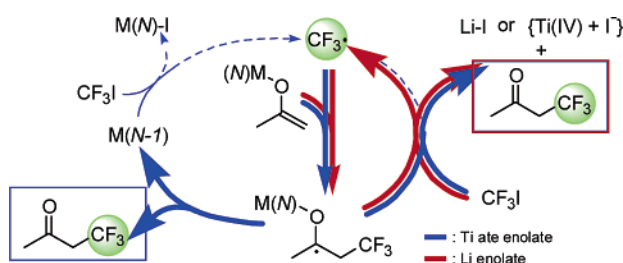
Experimental and Theoretical Studies on Radical Trifluoromethylation of Titanium Ate and Lithium Enolates

Yoshimitsu Itoh,[†] K. N. Houk,[‡] and Koichi Mikami^{*,†}

Department of Applied Chemistry, Tokyo Institute of Technology, Tokyo 152-8552, Japan, and Department of Chemistry and Biochemistry, University of California, Los Angeles, California 90095-1569

kmikami@o.cc.titech.ac.jp

Received August 3, 2006



The radical trifluoromethylation of Ti ate and Li enolates has been investigated by both experiments and density functional (UB3LYP/6-311+G**/UB3LYP/6-31+G*) calculations. Radical CF_3 addition to the enolates proceeds in a highly exothermic manner without significant reaction barriers in both Ti ate and Li enolates. There are two possible reaction paths after the addition of CF_3 radical in the case of Ti ate enolate; one is the elimination of Ti(III) from the ketyl radical intermediate and the other is the direct reaction of the ketyl radical intermediate with CF_3I . However, in the case of Li enolate, only the latter path is possible due to the high energy barrier of the elimination of the Li radical. This analysis provides an explanation of the experimental observation that the Li enolate could form the radical cycle efficiently but the Ti ate enolate could not. To make the radical cycle complete, I^- has to be extracted from CF_3I itself or the radical anion of CF_3I . In the case of Li, formation of Li–I bond could be the driving force for the extraction of I^- and regeneration of CF_3 radical. However, Ti does not give exothermic Ti–I formation and thus regeneration of CF_3 radical is less likely.

Introduction

Organofluorine compounds have attracted a great deal of attention because of their important applications in material and biological sciences. One of the most important organofluorine functionalities is CF_3 , which exhibits specific physical and biological properties.¹ The $\alpha\text{-CF}_3$ carbonyl compounds are useful synthetic intermediates for preparation of many derivatives containing the CF_3 group.

In sharp contrast to normal alkyl halides, trifluoromethyl (perfluoroalkyl) halides cannot undergo nucleophilic alkylation, because the electronegativities of perfluoroalkyl groups are higher than those of halogens and thus the polarization of perfluoroalkyl halides is as $\text{R}_f^{\delta-}-\text{I}^{\delta+}$. Treatment with nucleophiles does not produce $\text{R}_f\text{-Nu}$.² Therefore, introducing the CF_3 group by CF_3 radical addition to enolates is one of the most

straightforward and effective ways to obtain $\alpha\text{-CF}_3$ carbonyl compounds. We have been investigating radical trifluoromethylation of enolates, and the use of Ti ate enolates³ and Li enolates⁴

- (1) (a) Shimizu, M.; Hiyama, T. *Angew. Chem., Int. Ed.* **2005**, *44*, 214–231. (b) Ma, J.-A.; Cahard, D. *Chem. Rev.* **2004**, *104*, 6119–6146. (c) Mikami, K.; Itoh, Y.; Yamanaka, M. *Chem. Rev.* **2004**, *104*, 1–16. (d) Hiyama, T.; Kanie, K.; Kusumoto, T.; Morizawa, Y.; Shimizu, M. *Organofluorine Compounds*; Springer-Verlag: Berlin and Heidelberg, 2000. (e) Soloshonok, V. A., Ed.; *Enantiocontrolled Synthesis of Fluoro-Organic Compounds*; Wiley: Chichester, U.K., 1999. (f) Ramachandran, P. V., Ed.; *Asymmetric Fluoroorganic Chemistry, Synthesis, Applications, and Future Directions*; American Chemical Society: Washington, DC, 2000. (g) Chambers, R. D., Ed. *Organofluorine Chemistry*, Springer, Berlin, 1997. (h) Iseki, K. *Tetrahedron* **1998**, *54*, 13887–13914. (i) Ojima, I., McCarthy, J. R., Welch, J. T., Eds.; *Biomedical Frontiers of Fluorine Chemistry*; American Chemical Society: Washington, DC, 1996. (j) Smart, B. E., Ed.; *Chem. Rev.* **1996**, *96*, 1555–1824 (thematic issue on fluorine chemistry). (k) Banks, R. E., Smart, B. E., Tatlow, J. C., Eds.; *Organofluorine Chemistry: Principles and Commercial Applications*; Plenum Press: New York, 1994. (l) Hudlicky, M. *Chemistry of Organic Fluorine Compounds*, 2nd ed.; Ellis Horwood: Chichester, U.K., 1976.

[†] Tokyo Institute of Technology.

[‡] University of California, Los Angeles.

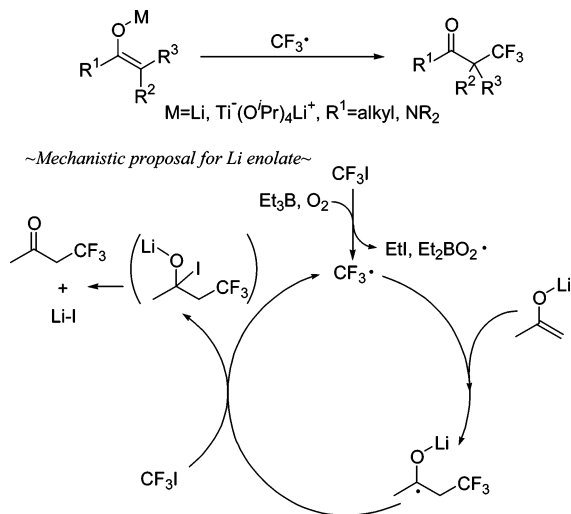


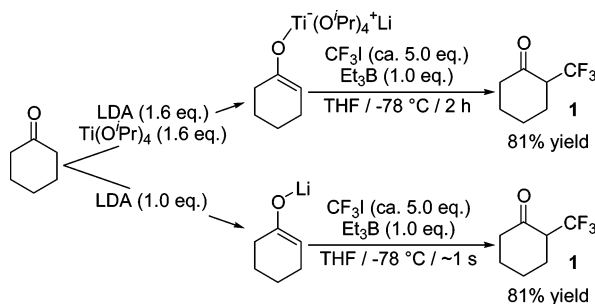
FIGURE 1. Previously proposed mechanism of the radical trifluoromethylation of Li enolates.

turned out to be an efficient way to synthesize α -CF₃ ketones. Except for our reports, there is only one example of the radical trifluoromethylation of Li enolates of imides by Iseki.^{5,6} For Li enolates, we and Iseki proposed similar mechanisms (Figure 1). However, no detailed investigation has been carried out from a mechanistic point of view. We report here the experimental and theoretical study of the mechanism of the radical trifluoromethylation of Ti ate and Li enolates.

Experimental Study

We have already reported that radical trifluoromethylation of Ti ate³ and Li enolates⁴ provides the α -CF₃ products in good yields (Scheme 1).

SCHEME 1



In investigating the amount of radical initiator (Et₃B), an interesting result was obtained. The relationship between the amount of Et₃B and the product yield is shown in Figure 2. In the case of Ti ate enolates, the yields gradually decreased as the amount of Et₃B decreased [LDA = Ti(OiPr)₄ = 1.0 and 1.6 equiv].⁷ In sharp contrast, this is not the case with Li enolates; α -CF₃ product could be obtained in good yield (71%) even when

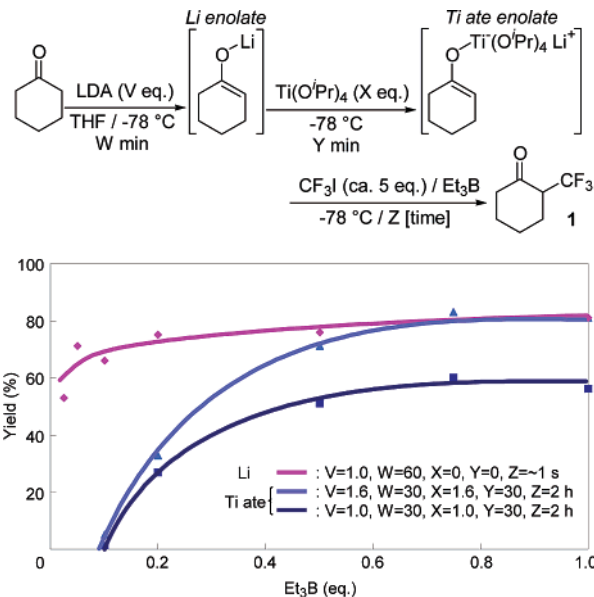


FIGURE 2. Relationship between the amount of Et₃B and the yields.

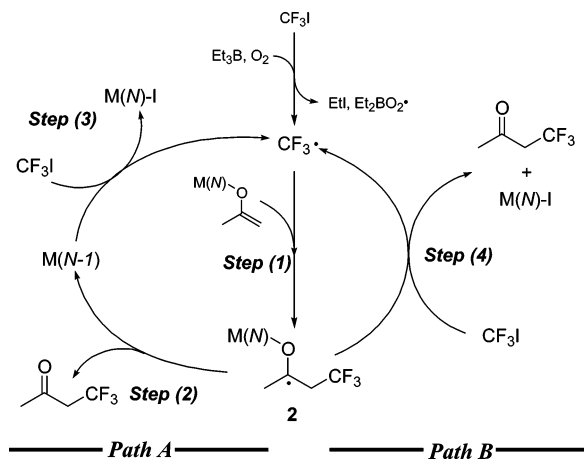


FIGURE 3. Proposed CF₃ radical addition mechanism.

the amount of Et₃B was reduced to 5 mol %. This indicates that the radical cycle does not work well for Ti ate enolate but does work well for Li enolate.

When the fact is considered that Ti has two stable oxidation states (III and IV), two reaction mechanisms could be proposed (Figure 3). First, CF₃ radical reacts with enolate (step 1). From the radical adduct (**2**), one possibility is path A: elimination of metal from ketyl radical intermediate (**2**) by reducing its

(6) Other examples of radical trifluoromethylation of enolate equivalents: (a) Perfluoroalkylation of silyl and germlyl enol ethers of esters and ketones: (i) Miura, K.; Taniguchi, M.; Nozaki, K.; Oshima, K.; Utimoto, K. *Tetrahedron Lett.* **1990**, *31*, 6391–6394. (ii) Miura, K.; Takeyama, Y.; Oshima, K.; Utimoto, K. *Bull. Chem. Soc. Jpn.* **1991**, *64*, 1542–1553. Perfluoroalkylation of silyl enol ethers provided the products in good yields except for trifluoromethylation. Trifluoromethylation of ketone germlyl enol ethers proceeds in good yield. (b) Trifluoromethylation of enamines: (i) Cantacuzène, D.; Wakselman, C.; Dorme, R. *J. Chem. Soc., Perkin Trans. I* **1977**, 1365–1371. (ii) Kitazume, T.; Ishikawa, N. *J. Am. Chem. Soc.* **1985**, *107*, 5186–5191.

(7) It is speculated that the Ti ate enolate is in equilibrium with the parent ketone and ate complex [LDA/Ti(OiPr)₄]. Although Ti ate enolate could be generated by using LDA = Ti(OiPr)₄ = 1.0 equiv, excess amount of LDA and Ti(OiPr)₄ [LDA = Ti(OiPr)₄ = 1.6 equiv] increases the yield of the α -CF₃ product, probably due to the equilibrium shift to the Ti ate enolate. See ref 2.

(2) (a) Huheey, J. E. *J. Phys. Chem.* **1965**, *69*, 3284–3291. (b) Yoshida, M.; Kamigata, N. *J. Fluorine Chem.* **1990**, *49*, 1–20.

(3) (a) Itoh, Y.; Mikami, K. *Org. Lett.* **2005**, *7*, 649–651. (b) Itoh, Y.; Mikami, K. *J. Fluorine Chem.* **2006**, *127*, 539–544.

(4) (a) Itoh, Y.; Mikami, K. *Org. Lett.* **2005**, *22*, 4883–4885. (b) Itoh, Y.; Mikami, K. *Tetrahedron* **2006**, *62*, 7199–7203.

(5) Trifluoromethylation of lithium enolate of imides: (a) Iseki, K.; Nagai, T.; Kobayashi, Y. *Tetrahedron Lett.* **1993**, *34*, 2169–2170. (b) Iseki, K.; Nagai, T.; Kobayashi, Y. *Tetrahedron: Asymmetry* **1994**, *5*, 961–974.

TABLE 1. Stabilization of Li Radical by Solvation

$$\cdot\text{Li} + n\text{Me}_2\text{O} \longrightarrow \cdot\text{Li}^{\oplus} \left(\text{O} \begin{array}{c} \diagup \\ \diagdown \end{array} \right)_n$$

| n | ΔE (kcal/mol) | ΔG (kcal/mol) |
|-------|-----------------------|-----------------------|
| 0 (3) | 0 | 0 |
| 1 (4) | -11.3 | -3.9 |
| 2 (5) | -19.8 | -2.6 |
| 3 (6) | -27.3 | 1.7 |
| 4 (7) | -35.3 | 6.4 |

oxidation number by 1, along with the formation of the α -CF₃ product (step 2). Regeneration of CF₃ radical can be achieved by the reaction of CF₃I with metal (step 3). Another possibility is path B, which is the same as Scheme 1; ketyl radical intermediate (2) directly reacts with CF₃I to regenerate CF₃ radical along with α -CF₃ product.

Theoretical Study

A computational study was carried out to evaluate the reaction mechanism and to uncover the origin of the difference between Ti ate and Li enolates.

Chemical Models and Computational Methods. For computational efficiency, lack of precise structural information on the reactive intermediate, and our qualitative goal, several simplifications were adopted: (1) Countercation (Li⁺) in Ti ate enolate was ignored. This simplification could be rationalized by the fact that there was no significant difference in the chemical yield upon addition of 12-crown-4.⁸ (2) Ti methoxide was adopted instead of the Ti isopropoxide actually used. (3) Aggregation was ignored.^{9,10} (4) Acetone was adopted as the substrate.

It is very important to consider the solvent, since all reactions were carried out in tetrahydrofuran (THF), and there are empty sites available on the metal for the coordination of THF to stabilize both the intermediate and the transition state. The usual maximum coordination number is four for Li and six for Ti. Therefore, in a preliminary study, stabilization energies of Li radical, Li⁺, Ti⁻(III)(OMe)₄, and Ti(IV)(OMe)₄ were investigated with dimethyl ether (Tables 1–4). All the structures were optimized at UB3LYP/631+LAN (LANL2DZ for Ti, 6-31+G* for others) level. Gibbs free energies (ΔG) contain zero-point, thermal, and entropy effects at 298.15 K and 1 atm pressure. In the case of Li, both radicals and cations are stabilized by coordination of ethers (Tables 1 and 2). One exception is ΔG of the Li radical; the first and second ethers stabilized the system but third and fourth ethers raised the energies slightly (Table 1, entries 3 and 4). This is due to the entropy effect. On the other

TABLE 2. Stabilization of Li⁺ by Solvation
$$\text{Li}^+ + n\text{Me}_2\text{O} \longrightarrow \text{Li}^{\oplus} \left(\text{O} \begin{array}{c} \diagup \\ \diagdown \end{array} \right)_n$$

| n | ΔE (kcal/mol) | ΔG (kcal/mol) |
|--------|-----------------------|-----------------------|
| 0 (8) | 0 | 0 |
| 1 (9) | -39.6 | -31.5 |
| 2 (10) | -73.2 | -54.3 |
| 3 (11) | -95.8 | -65.4 |
| 4 (12) | -109.4 | -67.3 |

TABLE 3. Stabilization of Ti⁻(III)(OMe)₄ by Solvation
$$\text{Ti}^-(\text{III})(\text{OMe})_4 + n\text{Me}_2\text{O} \longrightarrow (\text{MeO})_4\text{Ti}^-(\text{III}) \left(\text{O} \begin{array}{c} \diagup \\ \diagdown \end{array} \right)_n$$

| n | ΔE (kcal/mol) | ΔG (kcal/mol) |
|---------------------|-----------------------|-----------------------|
| 0 (13) | 0 | 0 |
| 1 | | |
| 2 (14) ^a | 25.9 | 40.4 |

^a Reference 11.

TABLE 4. Stabilization of Ti(IV)(OMe)₄ by Solvation
$$\text{Ti}(\text{IV})(\text{OMe})_4 + n\text{Me}_2\text{O} \longrightarrow (\text{MeO})_4\text{Ti}(\text{IV}) \left(\text{O} \begin{array}{c} \diagup \\ \diagdown \end{array} \right)_n$$

| n | ΔE (kcal/mol) | ΔG (kcal/mol) |
|---------------------|-----------------------|-----------------------|
| 0 (15) | 0 | 0 |
| 1 | | |
| 2 (16) ^a | 11.8 | 42.3 |

^a Reference 12.

hand, in the case of Ti, there was no stabilization by the coordination of ether (Tables 3 and 4). When the optimization was started with one ether, the ether dissociated as the optimization proceeded in both the Ti⁻(III) and Ti(IV) cases. When the optimization was started with two ethers, a hexacoordinated Ti complex was optimized, but the energy was higher than that of the noncoordinated species.

From these results, solvated models were constructed in the following manner: (1) The maximum allowed number of ether molecules was attached to the Li cation. (2) Solvent molecules were not attached for Ti species.

All the calculations were performed with the GAUSSIAN 03 program package.¹³ All the structures were optimized at UB3LYP/631+LAN (LANL2DZ for Ti, I, 6-31+G* for others)^{14,15} level. Then the energies were recalculated in the presence of polarizable dielectric (THF, $\epsilon = 7.58$) as described by the CPCM model¹⁶ at UB3LYP/631+LAN (LANL2DZ for

(8) 1,1,1-Trifluoro-4,4-dimethyl-5-phenyl-3-pentanone was used as a substrate. Ti ate enolate was prepared by LDA = Ti(OⁱPr)₄ = 1.0 equiv condition. The reaction was carried out at -78 °C for 2 h. The chemical yields were 52% (without 12-crown-4) and 53% (with 12-crown-4).

(9) Aggregation of Li enolates: (a) Jackman, L. M.; Lange, B. C. *Tetrahedron* **1977**, *33*, 2737–2769. (b) Williard, P. G.; Carpenter, G. B. *J. Am. Chem. Soc.* **1986**, *108*, 462–468. (c) Seebach, D. *Angew. Chem., Int. Ed. Engl.* **1988**, *27*, 1624–1654. (d) Abbotto, A.; Streitwieser, A.; Schleyer, P. v. R. *J. Am. Chem. Soc.* **1997**, *119*, 11255–11268. (e) Sun, X.; Collum, D. B. *J. Am. Chem. Soc.* **2000**, *122*, 2459–2463.

(10) Aggregation of Ti ate complexes: (a) Hampden-Smith, M. J.; Williams, D. S.; Rheingold, A. L. *Inorg. Chem.* **1990**, *29*, 4076–4081. (b) Kuhlman, R.; Vaartstra, B. A.; Streib, W. E.; Huffman, J. C.; Caulton, K. G. *Inorg. Chem.* **1993**, *32*, 1272–1278. (c) Boyle, T. J.; Alam, T. M.; Tafaya, C. J.; Mechenbier, E. R.; Ziller, J. W. *Inorg. Chem.* **1999**, *38*, 2422–2428. (d) Mehrotra, R. C.; Agrawal, M. M. *J. Chem. Soc. A* **1967**, 1026–1030.

(11) Structure **14** has an imaginary frequency (-8 cm⁻¹) corresponding to vibration of ether.

(12) Structure **16** has imaginary frequencies (-35, -28 cm⁻¹) corresponding to vibration of ether.

(13) Frisch, M. J., et al. Gaussian 03, Revision C.02; Gaussian, Inc.: Wallingford CT, 2004.

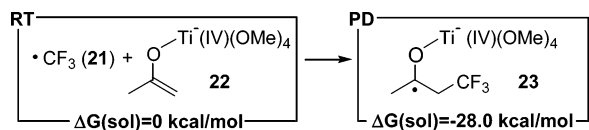
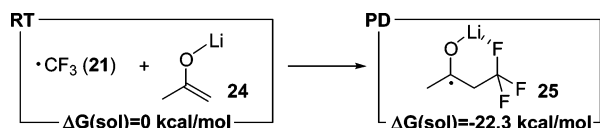
(14) B3LYP utilizes Becke's three-parameter exchange functional and the Lee–Yang–Parr correlation functional. (a) Becke, A. D. *Phys. Rev.* **1988**, *A38*, 3098–3100. (b) Becke, A. D. *J. Chem. Phys.* **1993**, *98*, 1372–1377. (c) Becke, A. D. *J. Chem. Phys.* **1993**, *98*, 5648–5652. (d) Lee, C.; Yang, W.; Parr, R. G. *Phys. Rev.* **1988**, *B37*, 785–788.

(15) (a) Hay, P. J.; Wadt, W. R. *J. Chem. Phys.* **1985**, *82*, 270–283. (b) Wadt, W. R.; Hay, P. J. *J. Chem. Phys.* **1985**, *82*, 284–298. (c) Hay, P. J.; Wadt, W. R. *J. Chem. Phys.* **1985**, *82*, 299–310. (d) Hehre, W. J.; Radom, L.; von Ragué Schleyer, P.; Pople, J. A. *Ab initio Molecular Orbital Theory*, Wiley: New York, 1986, and references therein.

TABLE 5. Calculated and Experimental Values of Electron Affinities of CF₃I and Benzophenone

| | method and basis set ^a | EA (eV) | |
|-------------------|-----------------------------------|---------|--------------------------|
| | | calc | exp |
| CF ₃ I | UB3LYP/631+LAN | 1.57 | 1.57 ± 0.2 ¹⁸ |
| CF ₃ I | UB3LYP/6311+LAN | 1.58 | |
| benzophenone | UB3LYP/631+LAN | 0.69 | 0.62 ± 0.1 ¹⁹ |
| benzophenone | UB3LYP/6311+LAN | 0.71 | |

^a All the structures were optimized at the UB3LYP/631+LAN level.

**FIGURE 4.** Step 1, Ti: CF₃ radical addition to Ti ate enolate.**FIGURE 5.** Step 1, Li: CF₃ radical addition to Li enolate (without solvent).

Ti, I, 6-311+G* for others) level. The energies shown in this report are Gibbs free energies and thus contain zero-point, thermal, and entropy effects at 195.15 K (experimental reaction temperature) and 1 atm pressure unless otherwise noted. The natural charges were calculated by the natural population analysis¹⁷ at the same level of the theory as the one used for geometry optimization.

To evaluate the calculation method, the electron affinities (EA) of CF₃I (neutral, **17**; radical anion, **18**) and benzophenone (neutral, **19**; radical anion, **20**) were calculated and compared with the experimental values (Table 5). The structures were optimized at the UB3LYP/631+LAN level, and energies were recalculated at the UB3LYP/6311+LAN level by use of the optimized geometry. Calculated EAs were comparable to the experimental values, giving some confidence in computational energetics.

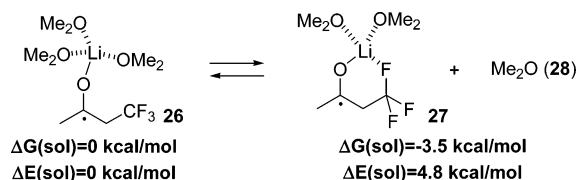
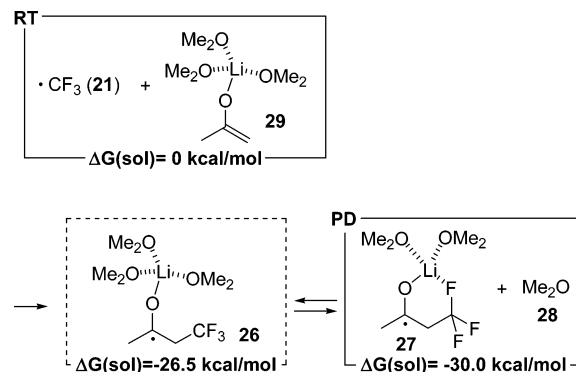
Results and Discussion

Step 1, Ti. As shown in Figure 4, CF₃ radical addition to Ti ate enolate is an exergonic reaction (−28.0 kcal/mol). A transition state could not be optimized; this reaction likely proceeds without a significant energy barrier.

Step 1, Li. The energetics for the reaction without solvent are shown in Figure 5. The reaction is exergonic, though slightly less (−22.3 kcal/mol). Li–F distance of the product (**25**) is 1.92 Å, which is shorter than the sum of the van der Waals radius of F and ionic radius of Li (2.08 Å), clearly showing the intramolecular coordination. Again a transition state could not be found.

(16) (a) Barone, V.; Cossi, M. *J. Phys. Chem. A* **1998**, *102*, 1995–2001. (b) Cossi, M.; Rega, N.; Scalamani, G.; Barone, V. *J. Comput. Chem.* **2003**, *24*, 669–681. (c) Klamt, A.; Schüürmann, G. *J. Chem. Soc., Perkin Trans. 2* **1993**, 799–805.

(17) Reed, A. E.; Weinstock, R. B.; Weinhold, F. *J. Chem. Phys.* **1985**, *83*, 735–746.

**FIGURE 6.** Comparison of radical intermediates with and without Li–F coordination.**FIGURE 7.** Step 1, Li: CF₃ radical addition to Li enolate (with solvent).

Without solvent, the coordination number of Li changes from one to two during the reaction. The Li on the product should have maximum coordination (four) to gain the highest stabilization by coordination. There are two possible product structures for four-coordinated Li. One structure has three ethers (**26**) and the other has ethers and intramolecular coordination with fluorine (**27**). Energies of these structures are compared in Figure 6. Compound **26**, which has no Li–F coordination, is less stable than coordinated **27** in terms of $\Delta G(\text{sol})$. However, when the optimization of **26** was started with Li–F coordination, Li and F gradually fell apart and the energy of **26** became more stable than **27** in terms of $\Delta E(\text{sol})$.²⁰ Initial product **26** is expected to form **27** to stabilize the system.

There are three vacant sites on Li in the substrate. Therefore, three ethers were attached to the substrate.²¹ The energetics for the solvated model of step 1 are shown in Figure 7. The reaction is also exergonic (−26.5 kcal/mol), and this value is almost the same as in the case of Ti.

Step 1, Naked Enolate. Energetics for naked enolate were also calculated (Figure 8). Again the reaction is exergonic (−24.9 kcal/mol) by about the same value as the other enolates.

This phenomenon was analyzed by charge distributions on the enolate. The charge distributions of enolates were calculated by natural population analyses and are listed in Table 6. All the enolates have a charge on the enolate part of more than −0.7, which shows that there is no significant difference between the metals on the enolates.

(18) Compton, R. N.; Reinhardt, P. W. *J. Chem. Phys.* **1978**, *68*, 4360–4367.

(19) Chowdhury, S.; Heinis, T.; Grimsrud, E. P.; Kebarle, P. *J. Phys. Chem.* **1986**, *90*, 2747–2752.

(20) This energy was obtained by UB3LYP/6-311+G**/UB3LYP/6-31+G* level theory. Single-point energy calculation was carried out in the presence of dielectric field (THF, $\epsilon = 7.58$), as described by the CPCMC model.

(21) Although it is known that π -enolate could be optimized and sometimes it is more stable than O-enolate in the case without solvent, O-enolate was adopted (which was first optimized) since the nonsolvated model is far from a realistic model compared to the solvated model. Getting further into the nonsolvated model is worthless in this study. See ref 9c.

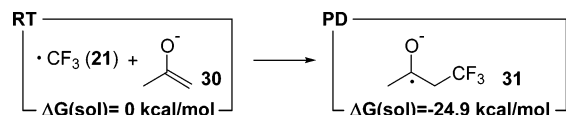


FIGURE 8. Step 1, no metal: CF_3 radical addition to naked enolate.

TABLE 6. Charge Distribution of Enolates

| enolates | natural charge | | $\Delta\Delta G(\text{sol})$ (kcal/mol) |
|-------------------------------------|----------------|---------|--|
| | metal | enolate | |
| Ti ate enolate (22) | -0.30 | -0.70 | -28.0 |
| Li enolate without solvent (24) | 0.96 | -0.96 | -22.3 |
| Li enolate with three solvents (29) | 0.94 | -0.94 | -26.5 |
| naked enolate (30) | 0 | -1 | -24.9 |

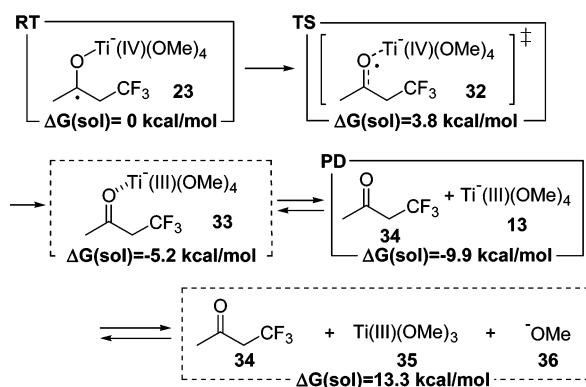


FIGURE 9. Step 2, Ti: Ti elimination from the radical intermediate.²²

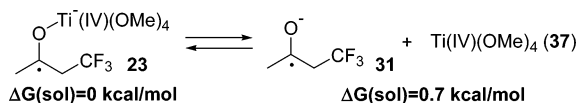


FIGURE 10. Dissociation of Ti(IV) from the radical intermediate.

Step 2, Ti. The energetics of step 2 including various forms of the product are shown in Figure 9. The transition state was also optimized. The activation free energy is relatively low (3.8 kcal/mol), and the reaction was slightly exergonic. Dissociation of ketone from Ti(III) lowers the energy to -9.9 kcal/mol. Dissociation of $-\text{OMe}$ from Ti(III) ate type complex is highly unfavorable and raises the energy by 23.2 kcal/mol.

There is a possibility of dissociation of $\text{Ti}(\text{IV})(\text{OMe})_4$ from **23**, leaving naked ketyl radical. Energetics for this dissociation are shown in Figure 10 and it is clear that dissociation of $\text{Ti}(\text{IV})$ is less thermodynamically favorable than $\text{Ti}(\text{III})$ elimination (0.7 vs -9.9 kcal/mol).

Step 2, Li. Energetics of the reaction without solvent are shown in Figure 11. The fluorine atom has a lone electron pair. The initial product involves coordination with the Li radical. The reaction is endergonic (28.3 kcal/mol). Dissociation of Li radical from $\alpha\text{-CF}_3$ ketone makes only a slight difference in the total energy (0.6 kcal/mol difference).

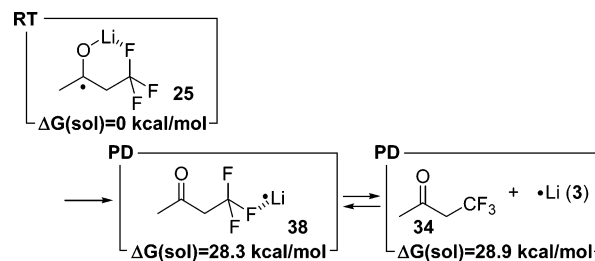


FIGURE 11. Step 2, Li: Li elimination from the radical intermediate (without solvent).

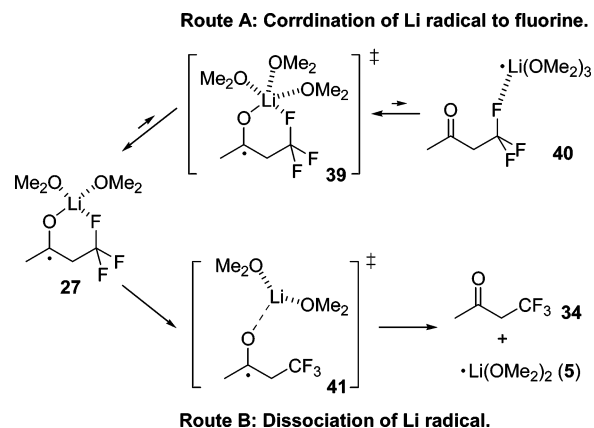


FIGURE 12. Two possible transition states for Li elimination.

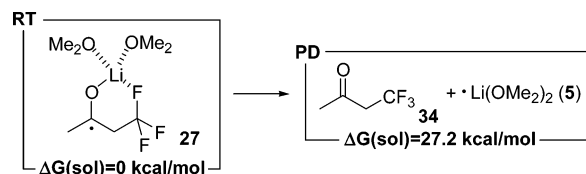


FIGURE 13. Step 2, Li: Li elimination from the radical intermediate.

When the solvated model is considered, two reaction paths are possible. In route A, the Li radical keeps the coordination with fluorine atom; in route B, Li radical completely dissociates from ketone (Figure 12). However, optimization of the product of route A (**40**) failed, since the spontaneous reduction of the carbonyl group leads to occupation of the vacant site of Li with ether.

The energetics of step 2 for Li are shown in Figure 13. This step is endergonic by 27.2 kcal/mol and, hence, probably unlikely to take place.

Step 3. There are two possible reaction paths for step 3: (a) electron transfer (denoted as ET) and (b) atom transfer (denoted as AT). These two pathways should be considered in both Ti and Li cases.

Step 3, Ti. The energetics for regeneration of CF_3 radical by $\text{Ti}(\text{III})$ are shown in Figure 14. The initial product of AT is the $\text{Ti}(\text{IV})$ ate complex and the CF_3 radical. The initial products of ET are $\text{Ti}(\text{IV})$ and radical anion of CF_3I . To regenerate CF_3 radical, I^- should dissociate from the radical anion of CF_3I . However, extraction of I^- by $\text{Ti}(\text{IV})$ is thermodynamically unfavorable (Figure 14A). Spontaneous dissociation of I^- from the radical anion of CF_3I is slightly unfavorable by 0.9 kcal/mol (Figure 14B). Overall, regeneration of CF_3 radical is unfavorable as experimentally observed.

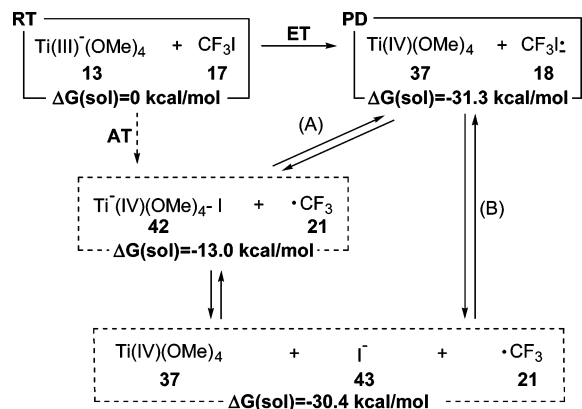


FIGURE 14. Step 3, Ti: Regeneration of CF_3 radical by Ti(III).

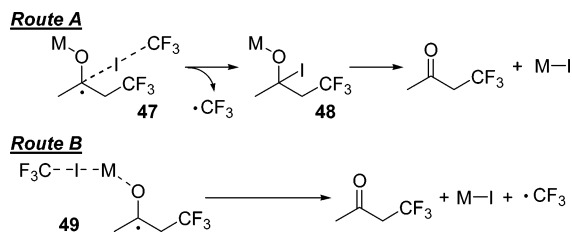


FIGURE 15. Two possible reaction pathways of AT for step 4.

Step 3, Li. Step 2 for Li (Figure 13) has a high reaction barrier. Step 3 hardly takes place.

Step 4. As in the case of path 3, there are two possible pathways, that is, ET and AT pathways.^{23,24} Furthermore, in AT, there are two possible routes: (A) C–I bond-forming path and (B) M–I bond-forming path (Figure 15). Route A involves α -iodoalkoxide intermediate **48**. Decomposition of **48** gives the α - CF_3 product. However, the structure **48** could not be optimized because I^- dissociates during the optimization, and no C–I bond was formed. This phenomenon was observed in both Ti and Li cases, indicating that route B would be favorable. However, distinction between routes A and B could not be well defined.

Step 4, Ti. Energetics of step 4 for Ti are shown in Figure 16. Regeneration of CF_3 radical is completed in one step in the case of AT. In the case that ET takes place, it requires at least one more step to regenerate CF_3 radical. Although the reaction is exergonic, regeneration of CF_3 radical is unfavorable. This trend is exactly the same as in step 3.

Step 4, Li. Energetics of the reaction without solvent are shown in Figure 17. The same trend as in step 3 is observed. In sharp contrast to Ti, regeneration of CF_3 radical from the ET

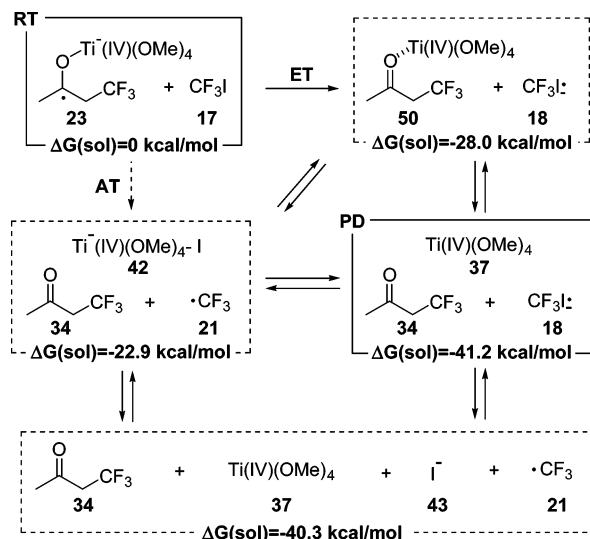


FIGURE 16. Step 4, Ti: Regeneration of CF_3 radical by radical intermediate.

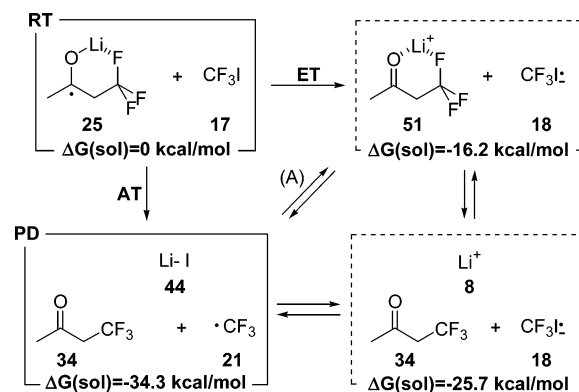


FIGURE 17. Step 4, Li: Regeneration of CF_3 radical by radical intermediate (without solvent).

product (**51**) is thermodynamically favorable because of exothermic Li–I bond formation. Iodide could be effectively extracted from the radical anion of CF_3I to regenerate CF_3 radical.

A solvated model was constructed by attaching two ethers on Li to fill up the empty site on Li. The result of the calculations is shown in Figure 18. Energetics are almost the same as for the nonsolvated model, and CF_3 radical could be regenerated by extraction of I^\bullet from CF_3I itself (AT) or of I^- from the radical anion of CF_3I (ET) by Li^+ , whichever route could regenerate CF_3 radical to make the radical cycle work well as experimentally observed.

Radical Anions of MeI and CF_3I . It is well-known that the radical anion of MeI (**55**) does not have a stable form and I^- will dissociate spontaneously (Figure 19).²⁶ For the radical anion of CF_3I ,²⁷ the strong electron-withdrawing nature of F stabilizes

(22) Structure **33** has an imaginary frequency (-29 cm^{-1}) corresponding to rotation of Me group on the ligand.

(23) Theoretical study of the reaction of ketyl radical and alkyl halide: (a) Sastry, G. N.; Shaik, S. *J. Am. Chem. Soc.* **1995**, *117*, 3290–3291. (b) Sastry, G. N.; Shaik, S. *J. Phys. Chem.* **1996**, *100*, 12241–12252. (c) Bertran, J.; Gallardo, I.; Moreno, M.; Savéant, J.-M. *J. Am. Chem. Soc.* **1996**, *118*, 5737–5744. (d) Sastry, G. N.; Danovich, D.; Shaik, S. *Angew. Chem., Int. Ed. Engl.* **1996**, *35*, 1098–1100. (e) Shaik, S.; Danovich, D.; Sastry, G. N.; Ayala, P. Y.; Schlegel, H. B. *J. Am. Chem. Soc.* **1997**, *119*, 9237–9245. (f) Yamataka, H.; Aida, M.; Dupuis, M. *Chem. Phys. Lett.* **1999**, *300*, 583–587. (g) Bakken, V.; Danovich, D.; Shaik, S.; Schlegel, H. B. *J. Am. Chem. Soc.* **2001**, *123*, 130–134.

(24) Experimental study of the reaction of ketyl radical and alkyl halide: (a) Kimura, N.; Takamuku, S.; *J. Am. Chem. Soc.* **1994**, *116*, 4087–4088. (b) Kimura, N.; Takamuku, S. *Bull. Chem. Soc. Jpn.* **1991**, *64*, 2433–2437.

(25) Structure **52** has an imaginary frequency (-17 cm^{-1}) corresponding to vibration of ether.

(26) (a) Rossi, R. A.; Pierini, A. B.; Palacios, S. M. In *Advances in Free Radical Chemistry*; Tanner, D. D., Ed.; Jai Press: London, 1990; Vol. 1, pp 193–252. (b) Bertran, J.; Gallardo, I.; Moreno, M.; Savéant, J.-M. *J. Am. Chem. Soc.* **1992**, *114*, 9576–9585. (c) Zhou, Z. Y.; Xing, Y. M. *J. Mol. Struct.* **2000**, *532*, 87–93. (d) Mariano, D.; Vera, A.; Pierini, B. *J. Phys. Org. Chem.* **2002**, *15*, 894–902.

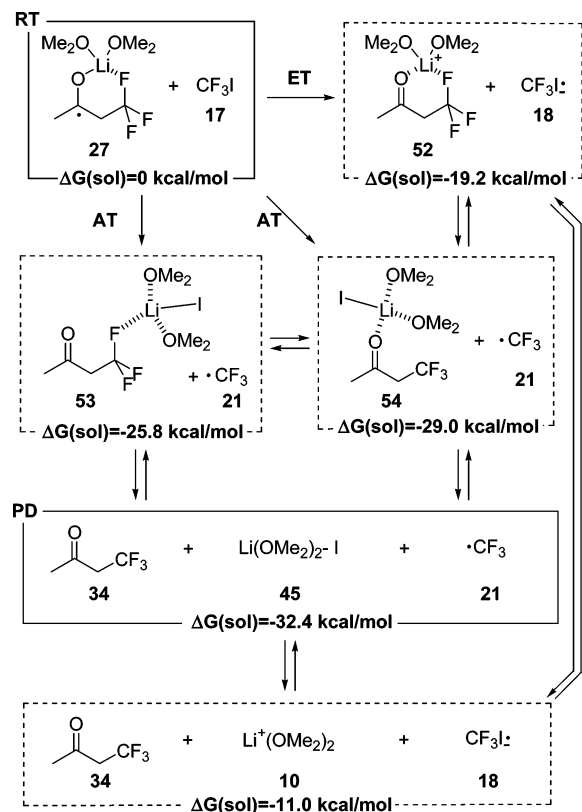


FIGURE 18. Step 4, Li: Regeneration of CF_3 radical by radical intermediate (with solvent).²⁵

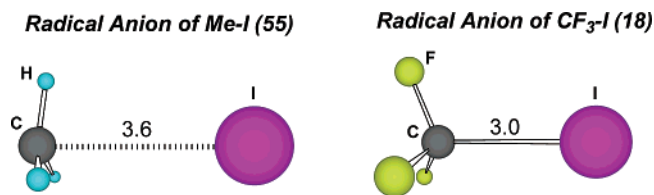


FIGURE 19. Structures of the radical anions of Me-I and $\text{CF}_3\text{-I}$ optimized at the UB3LYP/631+LAN level. Color representation of the atoms: black, carbon; blue, hydrogen; yellow, fluorine; magenta, iodine.

the anion species to prevent the spontaneous dissociation of I^- and, hence, the regeneration of CF_3 radical. This is the controlling factor of the effective radical cycle. Although there are two routes (ET and AT), I^* or I^- should be abstracted from CF_3I itself or the radical anion of CF_3I , respectively, to regenerate CF_3 radical. In the case of Li, Li^+ is favorable for bond formation with I^- but Ti(IV) is not.²⁸ This could be the rationale for Figure 2; Ti ate enolate requires equimolar amount of radical initiator and Li enolate requires only a catalytic amount thereof at the radical initiation step.

(27) Roszak, S.; Koski, W. S.; Kaufman, J. J.; Balasubramanian, K. J. *Chem. Phys.* **1997**, *106*, 7709–7713.

(28) It is known that when the structure optimization was carried out in the presence of dielectric field, the $\text{CF}_3\text{Cl} + \text{e}^- \rightarrow \text{CF}_3^* + \text{Cl}^-$ reaction appears as a concerted electron transfer-bond breaking process as in the case of alkyl halide (see ref 26b). However, there is extra driving force for the regeneration of CF_3 radical for Li^+ , which is Li-I bond formation, to facilitate the radical cycle. Therefore, even if the structure optimization was carried out in the presence of dielectric field, the major conclusion should not be changed.

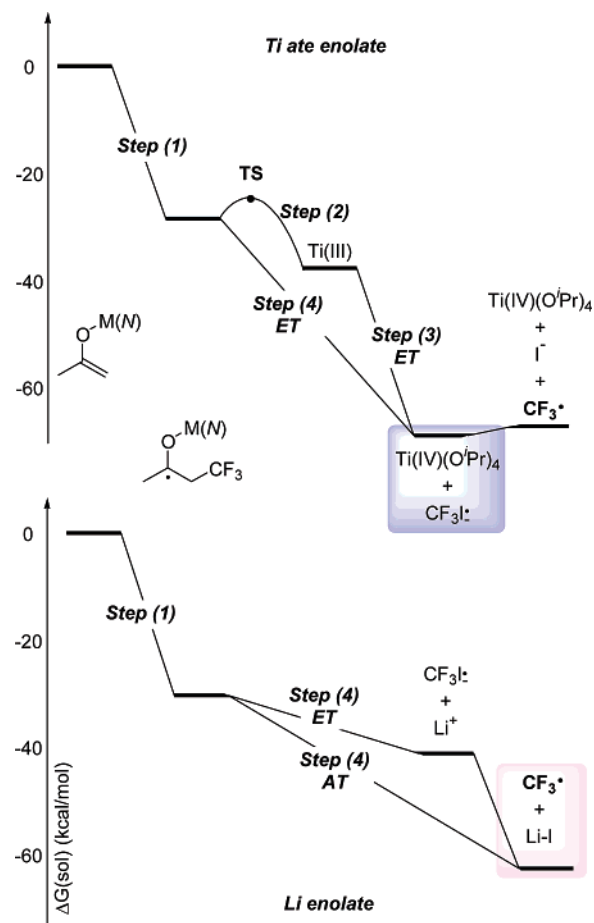


FIGURE 20. Energy diagram of radical trifluoromethylation of Ti ate and Li enolate.

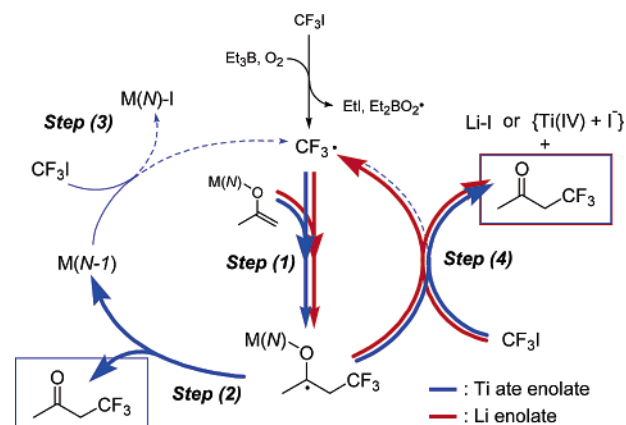


FIGURE 21. Reaction mechanism of radical trifluoromethylation of Ti ate and Li enolates.

Conclusion

An energy diagram of the reaction mechanism investigated above is shown in Figure 20, and a schematic reaction path is shown in Figure 21. In the case of Ti ate enolate, the CF_3 radical addition step (step 1) does not have a significant reaction barrier and thus occurs readily. Ti(IV) ketyl radical intermediate could proceed in either step 2 or step 4. For step 2, the reaction barrier is very low (3.8 kcal/mol). The Ti(III) species, which was generated after step 2, could react as a one-electron reductant to CF_3I but cannot abstract I^- from the radical anion of CF_3I to

regenerate CF_3 radical. Even when Ti(IV) ketyl radical proceeds to step 4, producing $\alpha\text{-CF}_3$ product, CF_3 radical could not be regenerated as in step 3. In the case of the Li enolate, the CF_3 radical addition step (step 1) does not have a significant reaction barrier. The difference between the reactions of Ti ate enolate and Li enolate could be found at step 2. Although the reaction barrier of step 2 of Ti(IV) ketyl radical is very low (3.8 kcal/mol), Li ketyl radical has a high reaction barrier (at least 27.2 kcal/mol) and thus Li ketyl radical would not proceed to step 2 but to step 4. Another difference between Ti and Li was observed at step 4. Li ketyl radical could react with CF_3I to produce $\alpha\text{-CF}_3$ product and Li^+ species. Li^+ could abstract I^- from the radical anion of CF_3I to regenerate CF_3 radical (ET). Another possibility is AT, which can regenerate CF_3 radical in one step. Effective regeneration of CF_3 radical is based on exothermic bond formation of Li-I in either (ET or AT) case. The difference between Ti ate enolate and Li enolate is attributed to the bondforming ability of the metal species with I^- to regenerate CF_3 radical (Figure 2).

Experimental Section

Typical Experimental Procedure for Radical Trifluoromethylation of Titanium Ate Enolate. To a solution of $^i\text{Pr}_2\text{NH}$ (44.9 μL , 0.32 mmol) in THF (2.0 mL) was added $^n\text{BuLi}$ (205.1 μL of 1.56 M solution in hexane, 0.32 mmol) at -78°C . The reaction mixture was stirred at 0°C for 30 min and then cooled to -78°C . To the solution was added cyclohexanone (20.7 μL , 0.2 mmol), and the mixture was stirred for 30 min at the temperature. Then $\text{Ti}(\text{O}^i\text{Pr})_4$ (94.5 μL , 0.32 mmol) was added to the solution. After the mixture was stirred for 30 min at -78°C , gaseous CF_3I (ca. 200 mg, ca. 1.0 mmol) was added with a cannula, followed by Et_3B (0.2 mL of 1.0 M solution in hexane, 0.2 mmol). The reaction mixture was stirred for 2 h at -78°C and then quenched by acetic acid (0.12 mL of 5 M solution in THF) at the temperature. After the mixture was warmed to room temperature, BTF (10 μL , 0.082

mmol) was added as an internal standard. The yield was determined by ^{19}F NMR of the crude mixture (81%).

Typical Experimental Procedure for Radical Trifluoromethylation of Lithium Enolate. To a solution of $^i\text{Pr}_2\text{NH}$ (28.0 μL , 0.20 mmol) in THF (2.0 mL) was added $^n\text{BuLi}$ (126.3 μL of 1.58 M solution in hexane, 0.20 mmol) at -78°C . The reaction mixture was stirred at 0°C for 30 min and then cooled to -78°C . To the solution was added cyclohexanone (20.7 μL , 0.2 mmol), and the mixture was stirred for 60 min at the temperature. Then, gaseous CF_3I (ca. 200 mg, ca. 1.0 mmol) was added with a cannula. Next, a syringe, which was filled with 0.12 mL of 5 M solution of acetic acid in THF, was set to the reaction vessel and kept untouched till the reaction was quenched. Then Et_3B (0.2 mL of 1.0 M solution in hexane, 0.2 mmol) was added in 15 s to start the radical addition reaction. The reaction mixture was immediately quenched (in ~ 1 s) by acetic acid solution, which was set beforehand, at -78°C . After the mixture was warmed to room temperature, BTF (10 μL , 0.082 mmol) was added as an internal standard. The yield was determined by ^{19}F NMR of the crude mixture (81%).

2-(Trifluoromethyl)cyclohexanone (1): ^1H NMR (CDCl_3 , 400 MHz) δ 1.62~1.88 (m, 3H), 1.92~2.14 (m, 2H), 2.24~2.39 (m, 2H), 2.42~2.53 (m, 1H), 2.98~3.13 (m, 1H). ^{13}C NMR (CDCl_3 , 75 Hz) δ 23.7, 27.1, 27.5 (q, $J = 2.4$ Hz), 42.2, 53.6 (q, $J = 25.7$ Hz), 124.6 (q, $J = 279.5$ Hz), 203.0. ^{19}F NMR (CDCl_3 , 376 Hz) δ -69.3 (d, 7.9 Hz) (ppm). IR (neat) 2954, 2876, 2364, 1729, 1272, 1170, 1125, 1060 (cm^{-1}). EI-MS $m/z = 166$ [M^+].

Acknowledgment. Generous allotment of computational time from the Institute for Molecular Science, Okazaki, Japan, is greatly acknowledged.

Supporting Information Available: General experimental procedure; Cartesian coordinates, total electron energies, and Gibbs energies for the optimized stationary points; and complete ref 13. This material is available free of charge via the Internet at <http://pubs.acs.org>.

JO0616153